Microstructure and electric properties of lead lanthanum titanate thin film under transverse electric fields

Z. T. Song[a)]
Department of Applied Physics and Materials Research Center, The Hong Kong Polytechnic University, Hung Hom, Kowloon, Hong Kong, China and State Key Laboratory of Functional Materials for Informatics, Shanghai Institute of Metallurgy, Chinese Academy of Sciences, 865 Changning RD, Shanghai, 200050, China

H. L. W. Chan, Y. P. Ding, N. Chong, and C. L. Choy
Department of Applied Physics and Materials Research Center, The Hong Kong Polytechnic University, Hung Hom, Kowloon, Hong Kong, China

Polycrystalline lead lanthanum titanate thin film having perovskite structure was fabricated by metalorganic deposition (MOD) on a $ZrO_2/SiO_2/Si$ substrate at 600 °C for 1 h in O_2 atmosphere. Columnar structured ZrO_2 buffer layer was also prepared by a MOD process under the same condition. Electrical measurements were conducted on interdigitated electrodes. The crystalline structure and growth behavior of the films have been studied by x-ray diffraction and scanning electron microscopy. It is observed that dielectric response of the film is effected by the cable length used in the measurement and by the values of the ac voltage. Long cable gives rise to an additional resonance peak at high frequency caused by the stray inductance of the contacts and cables. The capacitance and loss tangent over low frequency range shows significant variations due to the trapped charges and space charges in the film. These variations are very dependent on the values of the ac voltage and the length of cable. Meanwhile, the trapped charges and space charges lead to abnormal $P–E$ loops, in which the measured remanent polarization and coercive field increase with increasing frequency. © *2002 American Institute of Physics.* [DOI: 10.1063/1.1448867]

I. INTRODUCTION

Recently, ferroelectric thin films such as perovskite-structured compounds lead zirconate titanate(PZT) and lead lanthanum titanate (PLT) are considered to be promising not only for nonvolatile random access memories using their polarization reversal characteristics, but also for micromachined unimorph transducers in various microelectromechanical systems devices using their piezoelectric property.[1–4] Because the d_{33} and k_{33} values of most ceramics are almost two times that of the d_{31} and k_{31} values, respectively, unimorph bending actuators with a transversely polarized PZT layer have been prepared, which can be driven electromechanically through the piezoelectric d_{33} mode rather than the conventional d_{31} mode.[5] In this report, the lead titanate film doped with 10% La and with 10% Pb excess (PLT10) was deposited on ZrO_2-passivated silicon substrates, then interdigitated electrode was prepared on the surface. The crystallinity, microstructure, dielectric, and ferroelectric properties of the in-plane polarized film were investigated in detail.

II EXPERIMENTAL PROCEDURE

The ZrO_2 buffer layer and PLT10 thin film were prepared using a metalorganic deposition process by multiple spin-on procedures. The synthetic process of the metalalkoxide precursor solution have been described in detail elsewhere.[6,7] The substrate was a (100)-oriented n-type silicon wafers with a 5.46 μm-thick SiO_2 layer. The ZrO_2 layers were deposited on the substrate by spin coating using a photoresist spinner operated at 2500 rpm for 25 s. Each layer was pyrolyzed in O_2 at 600 °C for 10 min. After depositing 20 layers of ZrO_2, the resulting film was annealed in O_2 at 600 °C for 1 h. Another 20 layers of PLT10 were then spin coated and annealed in the same way as the ZrO_2 layers, and the final annealing condition was also in O_2 at 600 °C for 1 h.

The crystalline phase of the films was characterized by x-ray diffraction (XRD). The surface and cross section morphologies and thickness were evaluated by scanning electron microscopy [(SEM) Leica stereoscan 440]. Film roughness was determined by a stylus profilometry (Tencor P-10). The capacitance and dielectric loss curves were measured using a computer controlled impedance analyzer (HP4194A). The polarization–electric field ($P–E$) hysteresis loops were observed using a Sawyer–Tower circuit connected to a digital storage oscilloscope and an arbitrary function generator.

III RESULTS AND DISCUSSION

Figure 1(a) shows the XRD spectra of ZrO_2 film after being annealed in O_2 at 600 °C for 1 h. It is evident that tetragonal and monoclinic phases coexist in the film, but the tetragonal phase is the dominant one in the substrate. Figure

---

[a)]Present address: Business Department, Shanghai Institute of Metallurgy, Chinese Academy of Sciences, 865 Changning RD, Shanghai, 200050, China; electronic mail: ztsong@itsvr.sim.ac.cn
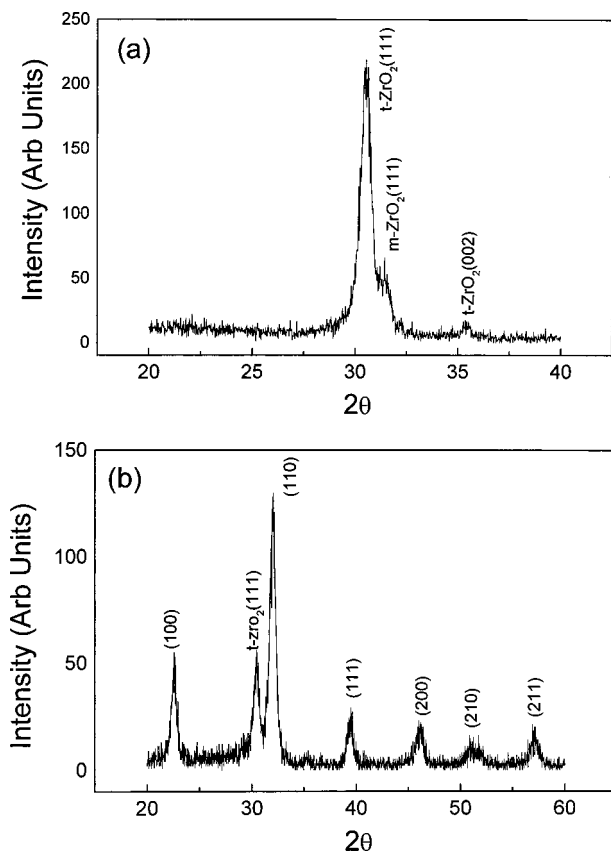
FIG. 1. XRD pattern of (a) ZrO_2 and (b) PLT10 films annealed by rapid thermal annealing process at 600 °C for 1 h in O_2.

FIG. 2. SEM micrograph of the (a) surface and (b) cross section of ZrO_2 film on SiO_2/Si(100) substrate.

1(b) shows that PLT10 film has a well-formed perovskite structure. The relevant intensities of the peaks are similar to those found in PLT10 ceramics, indicating that the crystallites in the film are randomly oriented.

Figure 2 shows the SEM micrograph of the (a) surface and (b) cross section of the ZrO_2 thin film after being annealed in O_2 at 600 °C for 1 h on the SiO_2/Si substrate. Figure 2 (a) shows that ZrO_2 film is dense and crack free, and has a relatively smooth surface. The surface average roughness of the film is 1.2 nm as measured by a stylus profilometry. Meanwhile, the grains in the film have a rather uniform size. In Fig. 2(b), the film was coated twenty times with a 0.2 M solution at 2500 rpm, and has a total thickness of 0.35 μm. This film consists of submicron sized columnar grains. Each layer exhibits a uniform and sharp interface.

The (a) surface and (b) cross sectional microstructures of the PLT10 film are shown in Fig. 3. Figure 3(a) shows that the PLT10 film was dense and crack free. The grains were round in shape and uniform in size ($\sim$50 nm). The surface average roughness of the film is 6.74 nm by a stylus profilometry. In Fig. 3(b), each layer of the structure was clearly observed and the thickness of PLT10 film is $\sim$0.67 μm. The amorphous SiO_2, columnar structured ZrO_2, and spherical PLT grains can be clearly seen.

In order to measure the electrical properties of the film under a transverse electric field, Cr/Au interdigitated electrodes (IDT) were sputtered on the surface of the PLT10 film. A conventional photoresist lif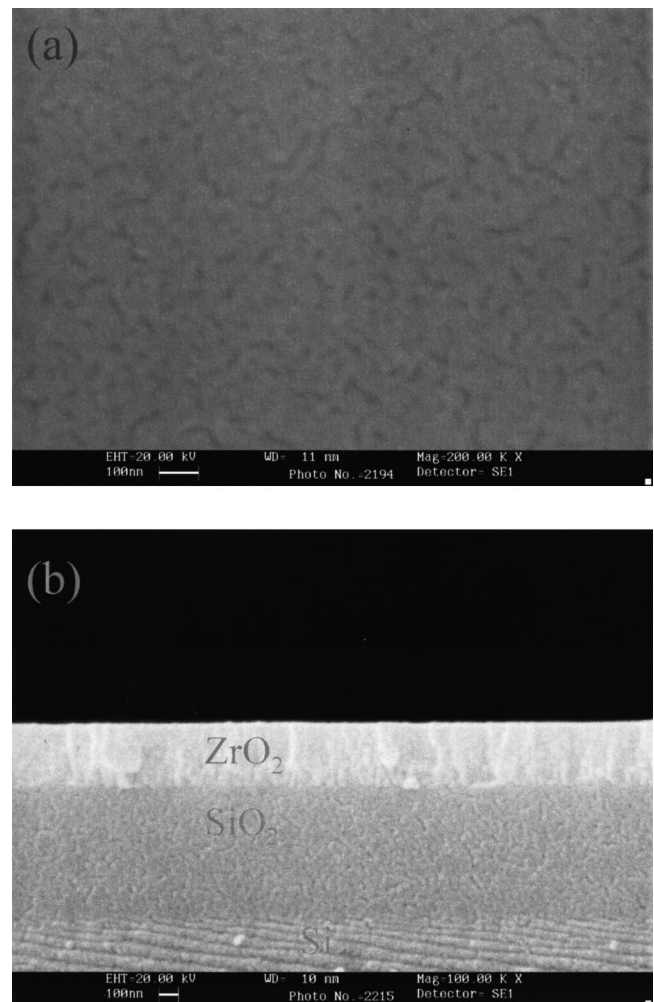t-off process was used to define the electrodes. The IDT had 22 pairs of electrodes with a finger width of 30 μm and a gap of 20 μm. The overlapping length was 620 μm as shown in Fig. 4.

The sample was connected to the impedance analyzer using two cables. The cables resistance is about 0.05 Ω/cm. Figures 5 and 6 show the frequency dependence of capacitance and loss tangent of the PLT10 film with an applied voltage of 1V ac and different length of cables. The frequency and length of cable were in the range of 100 Hz–40 MHz and 5–100 cm, respectively. It can be seen that the capacitance and loss tangent were very dependent on the length of cable. Resonance peaks can be clearly seen in Fig. 5. In the range of 100 H–1 kHz, the capacitance versus frequency shows significant variations which changes with the length of cable. With increase in the length of cable, the variations become more significant as shown in Fig. 5(b). In the range of 1 kHz to 1 MHz, [Fig. 5(c)], the capacitance measured using different length of cable did not change with frequency. With the increase in the length of cable, the capacitance are 36.6, 37.0, 37.1, 37.4, and 39.4 pF at 10 kHz, respectively as shown in Fig. 5(c). With the increase in frequency from 1 to 40 MHz, resonance peaks were observed around 10 MHz. The positions of these peaks changed with
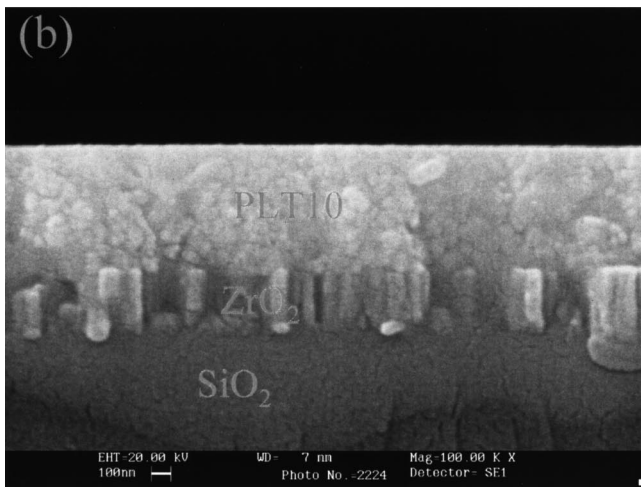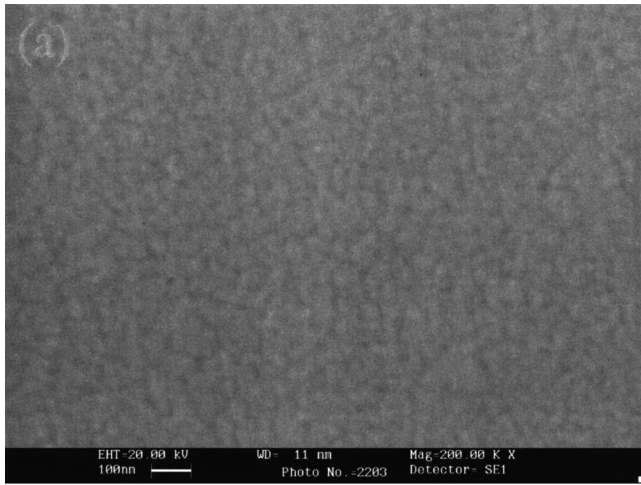
FIG. 5. Frequency dependence of capacitance of PLT10 film under a transverse electric field with different lengths of cable, the measurement frequency is in the range of 100 Hz–40 MHz.

ing relations with the capacitance curves. In the range of 100 Hz–4 kHz, the loss tangent shows significant scattering. With increase in frequency and decrease in the cable length, the scattering gradually decrease as shown in Fig. 6(b). In the range of 10 kHz–1 MHz, the loss tangent curves have no significant variation. With the increase in cable length, the loss tangent are 0.0058, 0.0034, 0.0017, 0.0025, and 0.0058 at 10 kHz, respectively as shown in Fig. 6(c). When f changes from 1 MHz to 40 MHz, resonance peaks occur at round 10 MHz. As l decreases, the resonance peaks move to higher frequency.

These results can be explained using an equivalent circuit as shown in Fig. 7. The sample can be represented by R_p and C in parallel and the cable and contacts can be represented by L and R_s in series. The total complex impedance can be written as:

$$Z = R_s + \frac{R_p}{1 + \omega^2 R_p^2 C^2} + j\frac{\omega L - \omega R_p^2 C + \omega^2 R_p^2 L C^2}{1 + \omega^2 R_p^2 C^2}. \quad (1)$$

The total capacitance being written as:

FIG. 3. SEM micrograph of the (a) surface and (b) cross section of PLT10 film on ZrO_2/SiO_2/Si(100) substrate.

the cable length l. The resonance peak appeared at 18 MHz when $l = 100$ cm. When $l = 50$ cm, the resonance peak was found at 24 MHz. For shorter cable length, the resonance peaks were found at f > 40 MHz. From Fig. 5(a) and 5(d), it can be clearly seen that the resonance peaks relate closely to the length of cable. With decrease in the cable length, the resonance peak moved to higher frequency. From Fig. 6, the loss tangent versus frequency curves have good correspond-
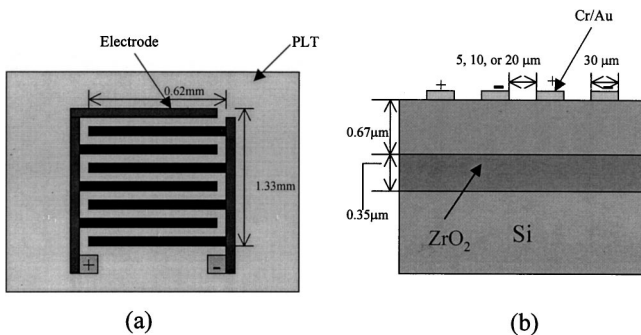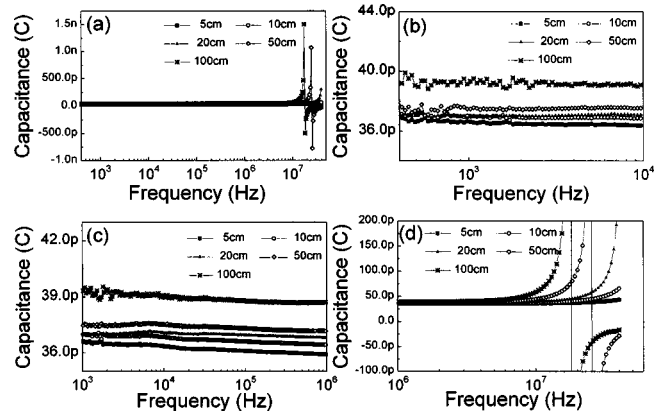

FIG. 4. Sketch of the interdigitated electrode pattern and film structure (a) top view and (b) cross sectional view.
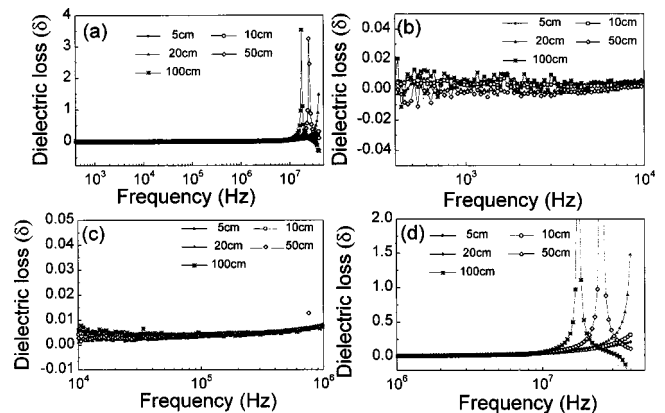

FIG. 6. Frequency dependence of loss tangent of PLT10 film under a transverse electric field with different length of cable, the measurement frequency is in the range of 100 Hz–40 MHz.

$$C_s = \frac{C + \dfrac{1}{R_p^2 \omega C}}{1 - \omega^2 LC \left(1 + \dfrac{1}{\omega^2 R_p^2 C^2}\right)} = \begin{vmatrix} C + \dfrac{1}{\omega^2 R_p^2 C} \;\ldots\ldots \text{(low-frequency)} \\[4mm] \dfrac{C}{1 - \omega^2 LC} \;\ldots\ldots\ldots\ldots \text{(Resonance)} \\[4mm] C \ldots\ldots\ldots\ldots\ldots\ldots\ldots (R_p = \infty; L = 0). \end{vmatrix} \tag{2}$$

The total loss tangent being written as:

$$tg\,\delta = \frac{\omega R_s\left(C + \dfrac{1}{\omega^2 R_p C}\right) + \dfrac{1}{\omega R_p C}}{1 - \omega^2 LC\left(1 + \dfrac{1}{\omega^2 R_p^2 C^2}\right)} = \begin{vmatrix} \dfrac{1}{\omega R_p C}\left(1 + \dfrac{R_s}{R_p}\right)\ldots\ldots\ldots\ldots\ldots\ldots\ldots\text{(low-frequency)} \\[4mm] \dfrac{\omega R_s\left(C + \dfrac{1}{\omega^2 R_p^2 C}\right) + \dfrac{1}{\omega R_p C}}{1 - \omega^2 LC}\left(\omega^2 \leqslant \dfrac{1}{LC}\right) \\[4mm] \dfrac{\omega R_s\left(C + \dfrac{1}{\omega^2 R_p^2 C}\right) + \dfrac{1}{\omega R_p C}}{\omega^2 LC - 1}\left(\omega^2 \geqslant \dfrac{1}{LC}\right)\ldots\text{(Resonance)} \\[4mm] \omega R_s C \ldots\ldots\ldots\ldots\ldots\ldots\ldots\ldots\ldots\ldots\ldots\ldots\ldots (R_p = \infty; L = 0) \end{vmatrix} \tag{3}$$

From these formulae, the stray inductance L of the contacts and cable may induce an L-C resonance at a resonant frequency f_r given by:

$$f_r = \frac{1}{2\pi\sqrt{LC}}. \tag{4}$$

With the decrease in the length of cable, the stray inductance L is decreased and the resonant frequency f_r increases. The high-frequency resonance peaks in Figs. 5 and 6 due to different length of cable may be explained by this L–C resonance.

From Eqs. (2) and (3), which suggest that C_s and $tg\,\delta$ are dependent on L and R_p, therefore, the capacitance curves decreases slightly with frequency as shown in Fig. 5(c). With decrease in the length of cable, the measured C_s is close to the sample capacitance.

The capacitance and loss tangent in between 100 Hz–1 kHz show significant scattering presumably due to the movement of space charges in the system.[8–11] There are three types of space charges in the PLT10 thin film. These include (1) the PLT10 dipoles , (2) ions of impurities, defects, vacancies, and (3) injected charges. In polycrystalline PLT10 film, the replacement of Pb^{+2} by La^{+3} leads to an excess positive charge and B-site vacancies were created[12] to maintain the electrical neutrality. These vacancies and other impurities exist in the grain, at intergrain boundaries or at interfaces and form various kinds of defects which trap charges in the PLT

FIG. 7. Equivalent circuit of the measured sample.

film. Therefore, the amount of charge traps and defect levels in the film are closely related to the grain size, the intergrain boundaries and the interface between the film and the electrode.[6,13] As the applied ac signal is well below the coercive field, hence, domain switching will not occur and the movement of the space charges will be the main cause of the scattering in the capacitance measurement at low frequencies. With a further increase in frequency, the trapped charges and space charges contribution became negligible as they can not respond fast enough. Therefore, the scattering disappeared with the increase in frequency.

As the voltage drop across a longer cable is higher, the effective voltage applied to the film becomes smaller and the scattering becomes more significant with the increase in cable length. It is thus seen that the scattering is also closely related to the voltage applied across the film. Figures 8 and 9 show the capacitance and loss tangent for 5 cm length of cable under different ac voltage. The frequency and ac signal were in the range of 100 Hz–40 MHz and 0.1–1 V, respectively. The capacitance and loss tangent show significant scattering in the range of 100 Hz–1 kHz. With decrease in the ac voltage, the scattering level became more significant as shown in Figs. 8(b) and 9(b). With increase in frequency, the scattering gradually disappeared. Cho found that capacitance increases with increase in ac oscillation voltage in the low frequency region.[8] This is due to domain switching as signal approaches the coercive field of the thin film. Our results are different from Cho's results as the electric field used in the present study is much lower than the coercive field. The curves over the low frequency range show significant variations due to the movement of space charges (ions of impurities, vacancies, etc.), in the film.[11] As the charges have to overcome the work function of the electrode in order to be injected into the film, hence, at low applied voltage, the amount of injected charges may be small. With the increase
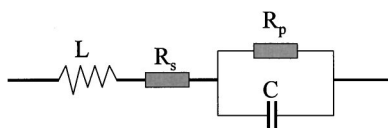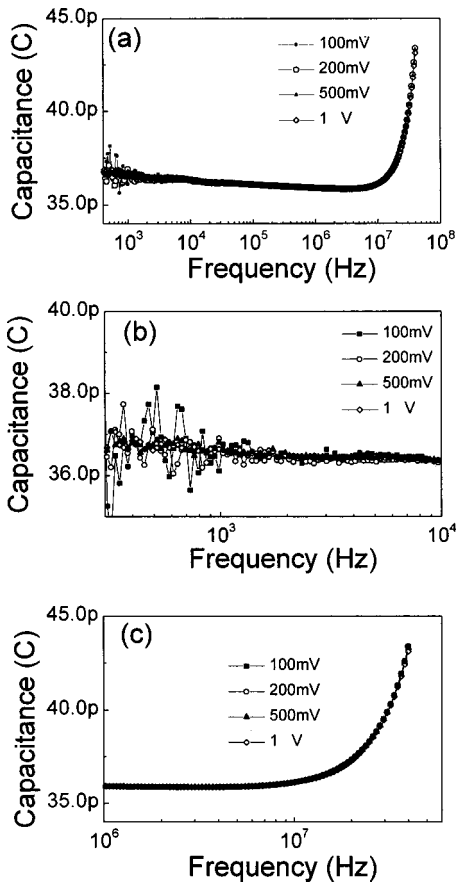
FIG. 8. Frequency dependence of capacitance and of PLT10 film under a transverse electric field with different small signal ac voltage, the measurement frequency is in the range of 100 Hz–40 MHz.
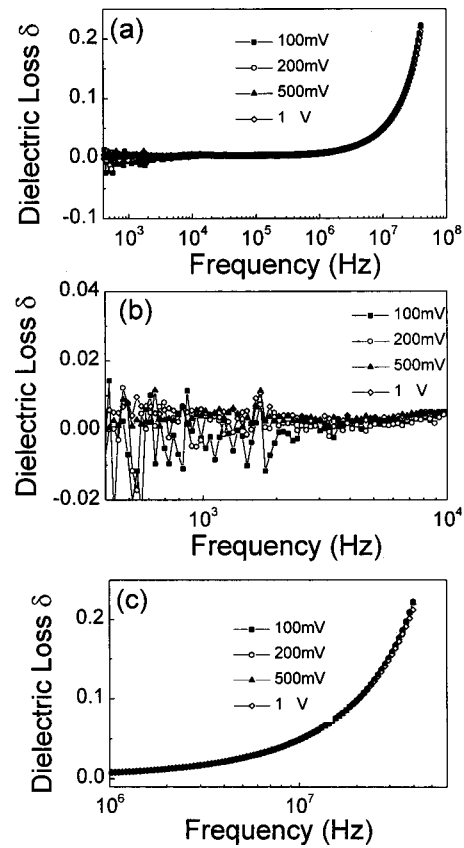

FIG. 9. Frequency dependence of loss tangent of PLT10 film under a transverse electric field with different small signal ac voltage, the measurement frequency is in the range of 100 Hz–40 MHz.

in the ac voltage, the increased amount of injected charges (which have the same sign as the charges on the electrode) and the ions or vacancies drifted towards the electrode under the electric field (with opposite sign to the injected charges) may effectively neutralized and the variation clearly became smaller.

In the IDT configuration, it is assumed that the area in which charge switching takes place is the product of the length of the electrode fingers and the film thickness and that the field is uniform across the electrode gap. Figure 10 shows a plot of the $P-E$ hysteresis loops measured as a function of applied voltage for the PLT10 film under transverse electric fields. The polarization and coercive electric field increase with increasing applied voltage, and the shape of the hysteresis loop was rather symmetric.

The frequency dependence of the $P-E$ hysteresis loop measured at 150 V is shown in Fig. 11. The remanent polariztion and the coercive field increase with increasing frequency and the shape of the hysteresis loop was symmetric. At 500 Hz, it is observed that the shape of the hysteresis loop is different from that of the loops measured at low frequencies. The remanent polarization and the coercive field usually were found to decrease with increasing frequency in a MFM capacitor configuration. which is due primarily to the basic limitation on the speed at which the domains can switch.[8,10] We obtained opposite results. As the IDT has large finger

width and gap (about 30 and 20 μm), with long finger length (620 μm and 22 pairs) and the applied electric field strength is not high enough to switch the dipoles, what is observed may be the injected space charges which cannot be discharged effectively as the frequency increases. These space charges take part in the switching and contribute to the increase in remanent polarization as shown in Figure 11.
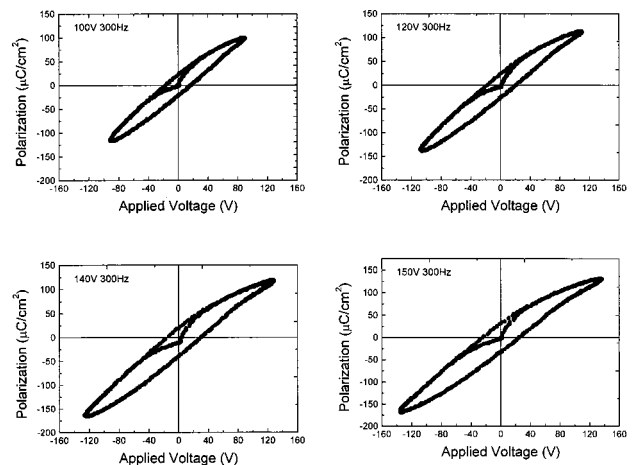

FIG. 10. Field-induced polarization for the interdigitated electrode pattern on the PLT10 film with frequency fixed at 300 Hz and applied voltage increased from 80 to 150 V.
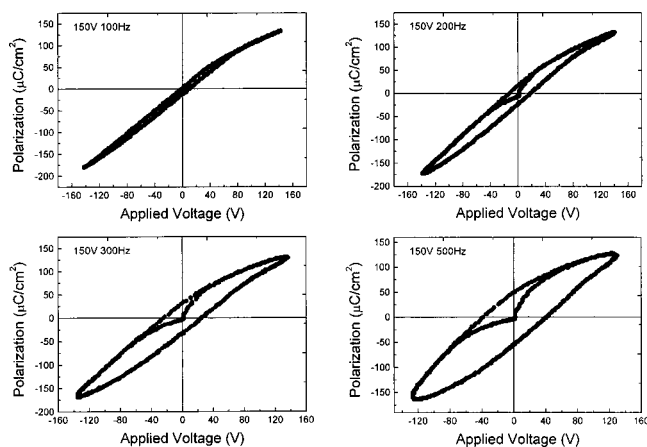
FIG. 11. Field-induced polarization for the interdigitated electrode pattern on the PLT10 film with applied voltage fixed at 150 V and frequency increased from 100 to 500 Hz.

IV. CONCLUSION

Polycrystalline PLT10 thin film exhibiting good perovskite structure. Columnar structured ZrO_2 can work effectively as a buffer layer. The surface morphology of ZrO_2 and PLT10 films were smooth with no cracks and defects while the grain size was uniform. The dielectric response of the film are very dependent on the length of cables and the magnitude of the ac voltage. The resonance peaks in the MHz region due to different length of cable were explained using a simple equivalent circuit model. The high frequency resonance peak was caused by the stray inductance of the contacts and the cables. The significant variations at low frequency were related to the space charges in the film. The scattering can be effectively decreased by decreasing the cable length and by increasing the ac voltage. The small signal capacitance and loss tangent at 10 kHz were about 36.6 pF and 0.0058, respectively. Meanwhile, the trapped charges and space charges lead to abnormal P–E loops in which the measured remanent polarization and coercive field increase with increasing frequency. The remanent polarization and coercive field at 300 Hz and 150V were 35 μC/cm^2 and 15 kV/cm, respectively.

[1] J. F. Scott and C. A. Araujo, Science **246**, 1400 (1989).
[2] S. J. Lee, K. Y. Kang, and S. K. Han, Appl. Phys. Lett. **72**, 299 (1998).
[3] B. M. Xu, Y. H. Ye, and L. E. Cross, Appl. Phys. Lett. **74**, 3549 (1999).
[4] A. J. Moulson and J. M. Herbert, *Electroceramics* (Chapman and Hall, London, 1990), Chap. 6.
[5] B. M. Xu, R. G. Polcawich, S. T. McKinstry, Y. H. Ye, and L. E. Cross, Appl. Phys. Lett. **75**, 4180 (1999).
[6] Z. T. Song, W. Ren, S. X. Wang, L. M. Wang, C. L. Lin, L. Y. Zhang, and X. Yao, J. Phys. D **33**, 764 (2000).
[7] Z. T. Song, N. Chong, H. L. W. Chan, and C. L. Choy, Appl. Phys. Lett. **79**, 668 (2001).
[8] C. R. Cho, W. J. Lee, B. G. Yu, and B. W. Kim, J. Appl. Phys. **86**, 2700 (1999).
[9] C. C. Chang and C. S. Tang, J. Appl. Phys. **87**, 3931 (2000).
[10] P. C. Joshi and S. B. Desu, J. Appl. Phys. **80**, 2349 (1996).
[11] M. Sayer, A. Mansingh, A. K. Arora, and A. Lo, Integr. Ferroelectr. **1**, 129 (1992).
[12] K. Hardt and D. Hennings, J. Am. Chem. Soc. **55**, 230 (1972).
[13] Z. T. Song, W. Ren, X. R. Fu, X. R. Zhu, C. L. Lin, and X. Yao, J. Phys.: Condens. Matter **13**, 155 (2001).